Eur. Phys. J. Special Topics **225**, 2717–2727 (2016)

DOI: 10.1140/epjst/e2015-50326-1

THE EUROPEAN PHYSICAL JOURNAL SPECIAL TOPICS

Regular Article

Localization and coherent states in a quantum DNLS trimer

Ricardo Martínez-Galicia[1] and Panayotis Panayotaros[2,a]

[1] Facultad de Química, Departamento de Matemáticas, Universidad Nacional Autónoma de México, 04510 México D. F., México
[2] Depto. Matemáticas y Mecánica, Instituto de Investigaciones en Matemáticas Aplicadas y en Sistemas, Universidad Nacional Autónoma de México, 01000 México D.F., México

Received 14 December 2015 / Received in final form 17 May 2016
Published online 22 November 2016

Abstract. We compare quantum states obtained from the integration of exact and approximate evolution equations for a quantized discrete nonlinear Schrödinger system (DNLS) with three lattice sites (trimer). The initial conditions are Glauber coherent states, and their projections to subspaces with a definite number of particles, and we are especially interested in coherent states that correspond to classical states that are in the neighborhood of breather solutions of the classical system. The breathers are well defined periodic orbits of the classical DNLS that we heuristically view as examples of spatially localized solutions. The two evolution equations give converging results in the subspaces with an increasing number of particles. This is no longer the case for normalized projections of Glauber states, where we see that the distance between the quantum states obtained by the exact and approximate equations shows recurrence phenomena that depend on the number of quanta and on the dynamical properties of the classical trajectory.

1 Introduction

Spatial localization of energy in nonlinear lattices has been the subject of intense research in recent decades, as the effects of discrete translation symmetry and nonlinearity become important in many systems that include photonic crystals, optical waveguide arrays, and molecular chains [10,22]. In the case of systems that are modeled by a discrete nonlinear Schrödinger (DNLS) equation, localization can be studied by examining special solutions such as breathers, and traveling waves. The dynamical properties of such solutions can give insight into many experimental observations, and have been studied in great mathematical detail, see e.g. [25,32,39]. The quantized system [10,36] has also been studied by many authors, and there are several ways to define spatial localization at the quantum level, see e.g. [4,11,13,33].

The general goal of this work is to understand the consequences of some recent results on localization of the classical DNLS systems to the quantized systems. The use of classical information to understand the quantum problem has been more effective

[a] e-mail: panos@mym.iimas.unam.mx

in some special cases where classical integrability, present in the two-site problem, or near-integrability, present in certain limits of the parameters, allow us to consider semiclassical quantization of classical solutions, see [2,13]. Also some authors have tried to define localization in purely quantum terms. For instance, in lattices with translational symmetry, the lack of localized eigenstates has led to a definition of localization in terms of level splitting of the lowest energies [4]. In the case of lattices without translation symmetry one can also study localized quantum eigenstates [11,33]. Another possible definition uses localized states in Hartree approximations [26].

Our approach in this paper is based on the use of the classical (Heisenberg group) coherent states, referred to also as Glauber states, see [16,23]. These states are labeled by points in the classical phase space, and it is natural to examine the quantum evolution of coherent states corresponding to classical initial conditions with different dynamical behaviors. In particular, we can examine the quantum evolution of coherent states obtained from classical initial conditions that belong to the neighborhood of invariant sets that we identify as spatially localized solutions. At the same time, we can also view the classical evolution of the coherent state labels as an approximation to the quantum evolution, see e.g. [12]. This classical description of the quantum evolution has been used extensively in the literature, and is in some special cases exact. In general, Hamilton's equations for the coherent state labels can be derived from the quantum system using a variational Ansatz. The coherent states constitute a set of trial functions with free parameters, and Hamilton's equations appear as the necessary condition for the minimization of a suitable functional that vanishes when the quantum evolution is exact, see [1,3,6]. This procedure does not imply that the classically evolved coherent states are close to the exact states in general, and the object of this paper to obtain some further quantitative information about this question for some special classical solutions. The classically evolved coherent states approximate the quantum evolution in the so-called classical limit for the problem, see e.g. [34,37,38]. This limit will not be considered here; we discuss this briefly in Sect. 4.

Also, as the DNLS system has a global phase symmetry, it is meaningful to ask similar questions for states with a fixed number of quanta; these subspaces are invariant under the quantum evolution. In this paper we work with normalized projections of the Glauber coherent states to subspaces with a fixed number of quanta. An alternative set of coherent states that can be used in these subspaces are $SU(f)$ coherent states, where f is the number of sites of the lattice, [6,37]. The connection of the present study to the $SU(f)$ coherent states is seen in Sect. 4.

In this paper we compare the exact and classical evolutions (as above) for some initial Glauber states corresponding to certain breather solutions of the the DNLS equation with three sites (trimer). The trimer system is the smallest nonintegrable DNLS lattice and its classical dynamics has been studied by several authors [5,17,20,21,27,28]. We consider parameter signs that correspond to the focusing case, with Dirichlet boundary conditions, as in [28]. We are especially interested in two types of breathers with special properties, one-peak breathers that correspond to the the maximum of the energy for fixed power and are stable, and certain two-peak breathers that are linearly unstable and whose energy corresponds to the transition from a disconnected to a connected energy hypersurface at fixed power, see [27]. These solutions are discussed in more detail in Sect. 2.

The classically and exactly evolved unnormalized fixed-number projections of the Glauber states become closer as the number of quanta is increased. This fact follows easily from the normalization of the Glauber states. The two evolutions are not however observed to converge for the normalized fixed-number projections of Glauber states as the number of particles is increased. In the case of the stable breathers and

their vicinity the distance between the two evolutions shows some recurrence to relatively small values. The minimum distance, as well as the approximate period of the return to these minima depend on the number of quanta, and seem to be robust under small changes in the initial condition. In the case of coherent states corresponding to the unstable two-peak breather and its vicinity, the distance of the two evolutions seems more irregular. Also the dependence of the distance on the initial condition is more pronounced in the vicinity of the unstable breather. The preliminary results here suggest that the classical coherent states can identify some localization features of the quantum system, even if the the two evolutions are not close. Possible explanations of some of the observed behaviors are briefly discussed in Sect. 4.

The paper is organized as follows. In Sect. 2 we describe the classical cubic DNLS system, define breather solutions, and review some of their properties. In Sect. 3 we introduce the quantum DNLS system. In Sect. 4 we define the coherent states and the two evolution rules we compare, and present and discuss our numerical results.

2 Discrete NLS equation and breathers

Consider a one-dimensional lattice of f sites whose positions are described in terms of the index j. Each site j is occupied by an anharmonic oscillator and its dynamics is given by the cubic discrete nonlinear Schrödinger equation (DNLS)

$$\frac{du_j}{dt} = -i\delta\left(\Delta u\right)_j - 2i|u_j|^2 u_j, \tag{1}$$

where t is the time variable, $u_j \in \mathbb{C}$ is the complex amplitude of the oscillator in the lattice site j, $j \in \{1, \ldots, f\}$, and δ is a real number that represents the constant coupling between neighboring sites. The discrete Laplacian Δ is defined by

$$\begin{aligned} \left(\Delta u\right)_j &= u_{j+1} + u_{j-1} - 2u_j, \quad j = 2, \ldots, f-1 \\ \left(\Delta u\right)_1 &= u_2 - 2u_1, \left(\Delta u\right)_f = u_{f-1} - 2u_f. \end{aligned} \tag{2}$$

The particular choices of $\left(\Delta u\right)_1$ and $\left(\Delta u\right)_f$ are analogous to imposing Dirichlet boundary conditions.

System (1) is equivalent to Hamilton's equations

$$\frac{du_j}{dt} = -i\frac{\partial H}{\partial u_j^*}, \tag{3}$$

where $j \in \{1, \ldots, f\}$. The Hamiltonian H is given by

$$H = -\delta\left(\sum_{j=1}^{f-1} |u_{j+1} - u_j|^2 + |u_1|^2 + |u_f|^2\right) + \sum_{j=1}^{f} |u_j|^4. \tag{4}$$

The *power* $P = \sum_{j=1}^{f} |u_j|^2$ and energy of the system, represented by the Hamiltonian H, are conserved quantities.

According to studies of classical dynamics, cases $f = 1$ (monomer) and $f = 2$ (dimer) are integrable, while the trimer $f = 3$ is nonintegrable [20].

Also, in this study we are interested in the case $\delta > 0$ (the "focusing" case in optics), where certain stable localized solutions are more robust, e.g. can be generalized to the infinite lattice for all $\delta > 0$, see [39], and the continuous limit, where the focusing cubic NLS has bright soliton solutions.

A *breather* solution of (1) is a periodic solution of the form

$$u_j = e^{-i\omega t} A_j, \tag{5}$$

with ω real, and $A = [A_1, \ldots, A_f] \in \mathbb{C}^f$ independent of time t. Substituting (5) in (1) we obtain that the A_j and ω satisfy the system of nonlinear equations,

$$-\omega A_j = -\delta \left(\Delta A\right)_j - 2|A_j|^2 A_j, \quad \sum_{j=1}^{f} |A_j|^2 = C, \quad j = 1, \ldots, f \tag{6}$$

for a fixed C. Alternatively we can also consider the f equations for the A_j, with ω fixed. Note that if A is a solution of (6) so is $e^{i\phi}A$, for any $\phi \in \mathbb{R}$ independent of j. In [28] it is shown that in the case of boundary conditions given by (2) all solutions of (6) are real, modulo a global phase. Periodic boundary conditions lead to more breather solutions, see [30,31], i.e. boundary conditions affect the dynamics, and we can expect that they lead to nonequivalent quantum dynamics as well.

By their definition, breather solutions are relative equilibria of the global phase rotation symmetry of (1). They are also fixed points of the dynamics on the reduced phase space, obtained by considering the sphere of points with fixed power and identifying points that are on the same orbit of the action of global phase change. The quotient space is the complex projective space $\mathbb{C}P^{f-1}$, see [17,27] for a recent studies of the dynamics of the trimer in $\mathbb{C}P^2$. Breathers can be therefore thought of as the simplest nontrivial solutions of the DNLS system. Some general features of the continuation and bifurcation of breathers, e.g. as we vary δ, can be seen in the simplest cases of two and three lattice sites, where we find fold and pitchfork bifurcations, see [5,21,28].

A related characterization of breathers is that they are critical points of the energy for fixed power. Breathers that are local extrema of the energy are expected to be linearly and nonlinearly (orbitally) stable. The case of the one-peak breathers considered for the quantized problem in Sect. 4. Analogous solutions exist for larger lattices, see e.g. [28], the limit of an infinite lattice [39], and periodic boundaries [30]. The energies of breathers are the only energies where the energy hypersurface at fixed power can change its topology, e.g. from a disconnected to a connected set. In [27] it is argued that this can happen at the energy of the two-peak unstable breathers that we consider in the quantum problem below. The change to a connected energy hypersurface could favor the spread of energy to more sites, however a more detailed study of the dynamics in the vicinity of that breather for the trimer suggested that the spread of the energy to the whole lattice needs energies that are quite far from the energy of the two-peak breather. The same study also showed recurrences to the vicinity of the unstable two-peak configuration, see [27]. These ideas about the role of the two-peak breathers require further study, and should be relevant to larger lattices. In the present study the two-peak breather is interesting as an example of an unstable solution whose local dynamics and recurrences are relatively well studied.

Breather solutions are also examples of solutions exhibiting spatial localization, i.e. in the case where the amplitude $|A_j|$ are much smaller away from some set of sites, e.g. of $O(\delta)$ if $|\delta|$ is assumed small, see [25]. For larger coupling δ, spatial localization is generally a heuristic notion in finite lattices, but becomes precise in the infinite lattice case, where we can look for breathers with amplitude A_j that vanishes at infinity. Also, the notion of $k-$peak solution, defined in the limit $\delta \to 0$ can be extended to larger $|\delta|$ breathers, provided that the branches can be indexed in a well-defined way by their $\delta = 0$ limits. This is apparently possible with Dirichlet boundary conditions, see [27,28].

3 Bosonic quantization of the DNLS Hamiltonian

We now define the quantum DNLS, following the standard (bosonic) quantization rules, see e.g. [10]. Specifically, let V is the complex span of the "occupation number" basis elements $|n_1, n_2, \ldots, n_f\rangle$, where $n_1, \ldots, n_f \geq 0$. V is the complex Hilbert space associated to a system of bosons (Fock space), and the $|n_1, \ldots, n_f\rangle$ are also assumed to be orthonormal basis states of V satisfying

$$\langle m_f, \ldots, m_1 | n_1, \ldots, n_f \rangle = \delta_{m_1 n_1} \ldots \delta_{m_f n_f}, \tag{7}$$

with $\delta_{m_i n_j}$ the Kronecker delta.

Under quantization, the amplitudes of the complex modes u_j^* y u_j of a model such as (1) are identified with the bosonic creation and annihilation operators, $B_j^\dagger$ y B_j, $j = 1, \ldots, f$ respectively, defined by

$$\begin{aligned} B_j^\dagger |n_1, n_2, \ldots, n_j, \ldots, n_f\rangle &= \sqrt{n_j + 1} |n_1, n_2, \ldots, n_j + 1, \ldots, n_f\rangle, \\ B_j |n_1, n_2, \ldots, n_j, \ldots, n_f\rangle &= \sqrt{n_j} |n_1, n_2, \ldots, n_j - 1, \ldots, n_f\rangle, \quad \text{if } n_j > 0, \\ B_j |n_1, n_2, \ldots, 0, \ldots, n_f\rangle &= 0 |n_1, n_2, \ldots, 0, \ldots, n_f\rangle. \end{aligned} \tag{8}$$

The classical Hamiltonian H of (4) is quantized using

$$\begin{aligned} |u_j|^2 &\to \frac{1}{2}\big(B_j^\dagger B_j + B_j B_j^\dagger\big), \\ |u_j|^4 &\to \frac{1}{6}\big(B_j^\dagger B_j^\dagger B_j B_j + B_j^\dagger B_j B_j^\dagger B_j + B_j^\dagger B_j B_j B_j^\dagger \\ &\quad + B_j B_j^\dagger B_j B_j^\dagger + B_j B_j B_j^\dagger B_j^\dagger + B_j B_j^\dagger B_j^\dagger B_j\big). \end{aligned} \tag{9}$$

Substituting in classical Hamiltonian (4), and using (9), (10) we have the quantized Hamiltonian operator

$$\hat{H} = (1 - 2\delta) \sum_{j=1}^{f} B_j^\dagger B_j + \sum_{j=1}^{f} B_j^\dagger B_j B_j^\dagger B_j + \delta \sum_{j=1}^{f} \big(B_j^\dagger B_{j+1} + B_j B_{j+1}^\dagger\big). \tag{10}$$

Similarly P is quantized to the operator $\hat{N}$ given by

$$\hat{N} = \sum_{j=1}^{f} B_j^\dagger B_j. \tag{11}$$

The dynamics of the quantum system is described by the Schrödinger equation

$$i \frac{\partial |\Psi(t)\rangle}{\partial t} = \hat{H} |\Psi(t)\rangle, \tag{12}$$

whose formal solution is

$$|\Psi(t)\rangle = e^{-iHt} |\Psi(0)\rangle, \tag{13}$$

with $|\Psi(0)\rangle$ the initial state.

We define V_n as the complex subspace of V of states spanned by $|n_1, \ldots, n_f\rangle$ such that $n_1 + \ldots n_f = n$. We have that $p = \dim V_n = \frac{(n+f-1)!}{(f-1)!n!}$, the number of ways that n quanta can be placed in a lattice of f sites.

We also have $[\hat{N}, \hat{H}] = 0$. This implies that the V_n are invariant under the evolution of the Schrödinger equation (12) and we can chose an eigenfunction $|\psi_n\rangle$ of $\hat{N}$ such that we also have

$$\hat{H}|\psi_n\rangle = E|\psi_n\rangle. \tag{14}$$

The matrix representation of $\hat{H}$ in the basis of V_n has the block diagonal form

$$\hat{H} = \begin{pmatrix} H_0 & 0 & & & & \\ 0 & H_1 & 0 & & & \\ & 0 & H_2 & 0 & & \\ & & \cdot & \cdot & & \\ & & & \cdot & \cdot & \\ & & & & \cdot & \cdot \end{pmatrix}, \tag{15}$$

i.e. H_n has entries $\langle \Psi_i|\hat{H}|\Psi_j\rangle$, with Ψ_i, Ψ_j elements of the occupation number basis of V_n.

4 Coherent states and quantum evolution.

Let $(\alpha) = (\alpha_1, \alpha_2, \ldots, \alpha_f) \in \mathbb{C}^f$. We define the Glauber coherent state $|\,(\alpha)\rangle$ associated to $(\alpha) \in \mathbb{C}^f$ as the state satisfying

$$\hat{B}_j|\,(\alpha)\rangle = \alpha_j|\,(\alpha)\rangle \tag{16}$$

for all $j = 1, 2, \ldots, f$. The normalized Glauber coherent state $|\,(\alpha)\rangle$ can be written explicitly in terms of the number states $|n\rangle$ as

$$\begin{aligned} |\,(\alpha)\rangle = {} & e^{-\frac{1}{2}\left(|\alpha_1|^2+|\alpha_2|^2+\cdots+|\alpha_f|^2\right)} \\ & \times \sum_{n_1=0}^{\infty}\sum_{n_2=0}^{\infty}\cdots\sum_{n_f=0}^{\infty} \frac{\alpha_1^{n_1}\alpha_2^{n_2}\ldots\alpha_f^{n_f}}{\sqrt{n_1!n_2!\ldots n_f!}}|n_1, n_2, \ldots, n_f\rangle, \end{aligned} \tag{17}$$

see e.g. [16,23].

Let $\alpha(0) = (\alpha_1(0), \ldots, \alpha_f(0)) \in \mathbb{C}^f$ and consider a coherent state given for $|(\alpha(0))\rangle$. Fix any $n \geq 0$, and let

$$|\Psi_n(t)\rangle = e^{-iHt}P_n|(a(0))\rangle \tag{18}$$

where P_n is the orthogonal projection to the subspace V_n. Therefore $|\Psi_n(t)\rangle$ describes the exact quantum evolution of $P_n|(\alpha(0))\rangle$ in the invariant subspace V_n.

Note that

$$\begin{aligned} P_n|(\alpha_1, \alpha_2, \ldots, \alpha_f)\rangle = {} & e^{-\frac{1}{2}\left(|\alpha_1|^2+|\alpha_2|^2+\cdots+|\alpha_f|^2\right)} \\ & \times \sum_{n_1+\cdots+n_f=n} \frac{\alpha_1^{n_1}\alpha_2^{n_2}\ldots\alpha_f^{n_f}}{\sqrt{n_1!n_2!\ldots n_f!}}|n_1 n_2 \ldots n_f\rangle. \end{aligned} \tag{19}$$

Also, the projected Glauber states $P_n|(\alpha)\rangle$ are, up to normalization, $SU(f)$ coherent states, see [6,37,38] and comments below.

Alternatively, let $\alpha(t)$ be solution of Hamilton's equations (3) at time t, with initial condition $\alpha(0)$, and let $|(a(t))\rangle$ be the corresponding coherent state. Then let $|\tilde{\Psi}(t)\rangle = |(\alpha(t))\rangle$, and

$$|\tilde{\Psi}_n(t)\rangle = P_n|(\alpha(t))\rangle. \tag{20}$$

Thus (20) gives a "classical" approximation to the evolution of the projection of a coherent state, assuming it remains a coherent state. Reference [12] also describes "semiclassical" corrections to the Hamiltonian that are not considered here.

Hamilton's equations for the parameters of the Glauber coherent states (and analogues for more general sets of trial functions) can been derived from the Schrödinger equation by minimizing suitable functionals of the evolving states that vanish when the quantum evolution is exact, see [1,3,6] for precise definitions. Such derivations of Hamilton's equations for the parameters of the Glauber states do not imply automatically that the two rules give nearby trajectories. This scenario is realized in some special limits, such as the classical limit briefly discussed below. Also, in the original applications of coherent states, e.g. in [16], the classical evolution of the parameters gives the exact quantum evolution.

To compare the two rules of evolution above we measure the distance between the two states $|\Psi_n(t)\rangle$ and $|\tilde{\Psi}_n(t)\rangle$, that is

$$D(t) = \inf_{\phi\in\mathbb{R}} \| e^{i\phi}|\Psi_n(t)\rangle - |\tilde{\Psi}_n(t)\rangle\|^2. \tag{21}$$

The orthogonality between the subspaces V_n implies that

$$\inf_{\phi\in\mathbb{R}} \| e^{i\phi}|\Psi(t)\rangle - |\tilde{\Psi}(t)\rangle\|^2 \geq \sum_{n=0}^{\infty} \inf_{\phi_n\in\mathbb{R}} \| e^{i\phi_n}|\Psi_n(t)\rangle - |\tilde{\Psi}_n(t)\rangle\|^2, \tag{22}$$

therefore the $D(t)$ of (21) for different n can be used to estimate from below the difference between the two evolution rules for the initial condition $|\Psi(0)\rangle = |(\alpha(0))\rangle$.

Note that since the Glauber states are normalized, given a classical initial condition $\alpha(0)$, and a time t, the norms of each of the corresponding $|\Psi_n(t)\rangle$, $|\tilde{\Psi}_n(t)\rangle$ in the subspaces V_n must eventually vanish as $n \to \infty$. This implies that $D(t)$ must vanish as $n \to \infty$. This decay is observed to be rapid and monotonic in n in the examples we have examined, and will be reported elsewhere.

Also, we can consider the two evolutions for the normalized projections of $|\Psi(0)\rangle$ to each V_n. Such initial conditions correspond to quantum states with a definite number n of quanta. The difference between the two evolutions of the normalized state in V_n is then measured by

$$\overline{D}(t) = \| \ |\Psi_n(0)\rangle \ \|^{-2} \ D(t). \tag{23}$$

The relation between projected Glauber states $P_n|(\alpha)\rangle$, $\alpha \in \mathbb{C}^f$, and $SU(f)$ coherent states, see [6,37,38], is given by

$$P_n|(\alpha)\rangle = e^{-P(\alpha)/2} \frac{[P(\alpha)]^{n/2}}{\sqrt{n!}} |n;\xi\rangle, \quad \text{with} \quad \xi = [P(\alpha)]^{-1/2}\alpha, \tag{24}$$

where $|n;\xi\rangle$ denotes an $SU(f)$ coherent state in V_n, see [6], up to fixing a global phase convention for ξ, e.g. $\xi_1 = \xi_1^*$, see [37]. The fact that $P(\xi) = 1$ implies that the state $|n;\xi\rangle$ is normalized, see [6]. The normalized projected Glauber states initial conditions in (23) are therefore $SU(f)$ coherent states.

In what follows we present preliminary numerical results for the evolution of $\overline{D}(t)$ for a lattice with $f = 3$ sites for different coherent state initial conditions.

Figure 1(a) corresponds to to the quantum state $|(\alpha(0))\rangle$, where $\alpha(0)$ is the classical state $\mathcal{A}_1 = (0,1,0)$ that is completely localized at the site $j = 2$. The number of bosons is $n = 3$ and $\delta = 0.3$. The vertical axis is the difference $\overline{D}(t)$ while the horizontal axis is time t. Figure 1(b) is obtained from the same initial quantum state projected to the subspace of $n = 10$ bosons.

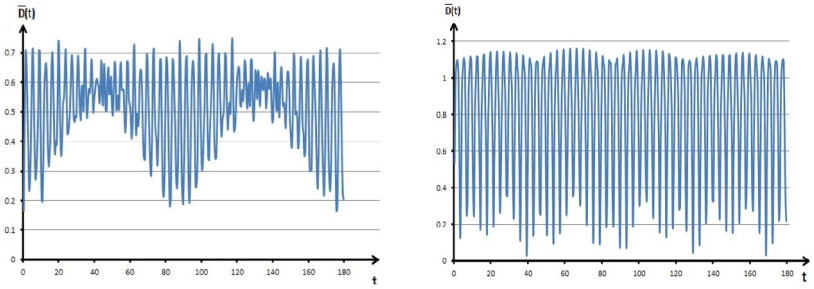

(a) (b)

Fig. 1. (a) $\overline{D}$ vs. t, initial condition is the normalized projected Glauber state corresponding to the classical state $\mathcal{A}_1 = (0, 1, 0)$, for $n = 3$ bosons, $f = 3$ sites, $\delta = 0.3$, $P = 1$. (b) $\overline{D}$ vs. t, initial condition is the normalized projected Glauber state corresponding to $\mathcal{A}_1 = (0, 1, 0)$, for $n = 10$ bosons, $f = 3$ sites, $\delta = 0.3$.

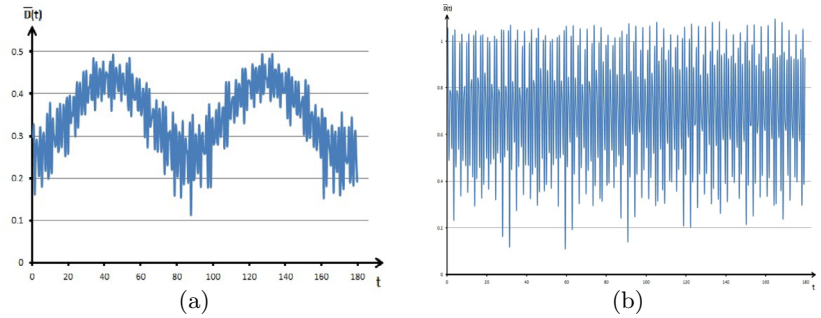

(a) (b)

Fig. 2. (a) $\overline{D}$ vs. t, initial condition is the normalized projected Glauber state corresponding to the classical initial condition $\mathcal{A}_2 = (0.149791, 0.977305, 0.149791)$, for $n = 3$ bosons, $f = 3$ sites, $\delta = 0.3$, $P = 1$. (b) $\overline{D}$ vs. t, initial condition is the normalized projected Glauber state corresponding to the classical initial condition $\mathcal{A}_2 = (0.149791, 0.977305, 0.149791)$, for $n = 10$ bosons, $f = 3$ sites, $\delta = 0.3$.

We see that $\overline{D}(t)$ varies in the range $[0.2, 0.7]$ for $n = 3$, and in the range $[0.03, 1.2]$ for $n = 10$. This indicates that the evolution rules for normalized projected coherent states do not convergence for large n. As indicated in the the two figures, as the number of bosons increases the minima of $\overline{D}(t)$ decrease, e.g. at $n = 10$ we see local minima of about 0.03, moreover the times between the minima decrease. These properties we seen in runs with up to $n = 30$ quanta.

Figures 2(a) and 2(b) correspond to the quantum state $|(\alpha(0))\rangle$, where $\alpha(0)$ is the breather $\mathcal{A}_2 = (0.149791, 0.977305, 0.149791)$, for $n = 3$, and $n = 10$ bosons respectively. We use $\delta = 0.3$. The breather $\mathcal{A}_2$ is a numerically computed solution of (6) with $P = 1$, and has period $T = 4.480916$. It corresponds to the point of maximum energy at $P = 1$, and is linearly and nonlinearly stable, see [27].

The behavior is qualitatively similar to the previous example, and the normalized distance $\overline{D}(t)$ varies in the range $[0.16, 0.46]$ for $n = 3$, and in the range $[0.1, 1.1]$ for $n = 10$. For $n = 10$ we see a recurrence to the local minimum value of about 0.3 at times separated by intervals that are comparable to the period of the breather. For $n = 3$ we see a less frequent recurrence.

Note that a classically evolved Glauber state $|\tilde{\Psi}(t)\rangle$, with initial condition $\tilde{\Psi}(0) = |(A)\rangle$, A a breather, has period T, where T is the period of the breather. The projections to each V_n, $n \geq 1$, have period T/n.

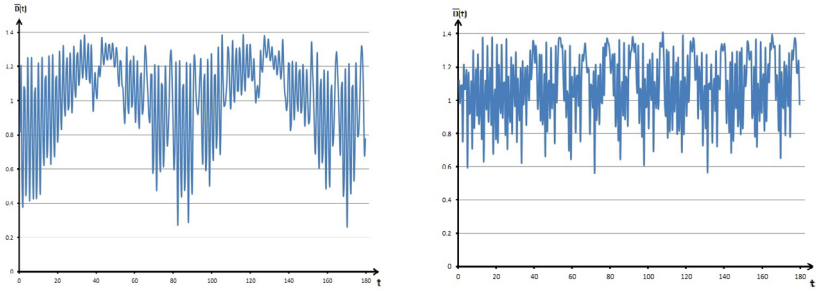

(a) (b)

Fig. 3. (a) $\overline{D}$ vs. t, initial condition is the normalized projected Glauber state corresponding to the classical state $\mathcal{A}_3(0) = (0.71607, 0.678973, 0.161982)$, for $n = 3$ bosons, $f = 3$ lattice sites, $\delta = 0.3$. (b) $\overline{D}$ vs. t, initial condition is the normalized projected Glauber state corresponding to the classical state $\mathcal{A}_3(0) = (0.71607, 0.678973, 0.161982)$ for $n = 10$ bosons, $f = 3$ sites, $\delta = 0.3$.

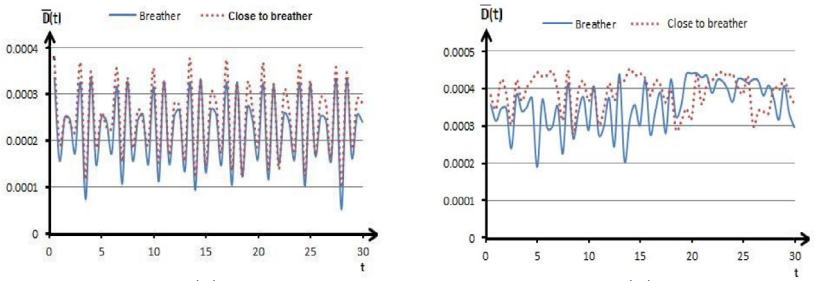

(a) (b)

Fig. 4. (a) Comparison of $\overline{D}$ vs. t for initial conditions that are normalized projected Glauber states corresponding to the classical state $\mathcal{A}_2$ (point on stable breather orbit), and $\mathcal{A}_2{}'$ (nearby point), for $n = 10$ bosons, $f = 3$ sites, $\delta = 0.3$. (b) Comparison of $\overline{D}$ vs. t for initial conditions that are normalized projected Glauber states corresponding to the classical state $\mathcal{A}_3$ (point on unstable breather orbit), and $\mathcal{A}_3{}'$ (nearby point), for $n = 10$ bosons, $f = 3$ sites, $\delta = 0.3$.

Figures 3(a) and 3(b) correspond to the quantum state $|(\alpha(0))\rangle$, where $\alpha(0)$ is the breather $\mathcal{A}_3 = (0.71607, 0.678973, 0.161982)$ with $n = 3$, and $n = 10$ bosons respectively. The period of the breather is $T = 8.849906$, and $\delta = 0.3$. $\mathcal{A}_3$ is a numerically computed solution of (6) with $P = 1$. It is the two-peak solution expected to correspond to the change from a connected to a disconnected energy hypersurface at $P = 1$, and is linearly unstable [27]. The normalized distance $\overline{D}(t)$ is in the range $[0.3, 1.4]$ for $n = 3$, and $[0.6, 1.4]$ for $n = 10$. In this case the local minima of $D(t)$ do not seem to decrease with n.

Figure 4(a) compares $\overline{D}(t)$ for normalized projected coherent states corresponding to $\mathcal{A}_2$ and a nearby initial condition $\mathcal{A}_2{}'$, while Fig. 4 (b) compares $\overline{D}(t)$ for the coherent states corresponding to $\mathcal{A}_3$ and a nearby initial condition $\mathcal{A}_3{}'$. In the case of the stable breather, $\overline{D}(t)$ for the two trajectories is close and exhibits the same recurrences. In the case of the unstable breather, $\overline{D}(t)$ appears to be more sensitive to the initial condition.

The above gives us a quantitative sense of the difference of the quantum and classical evolutions in a small lattice, and for the parameter regimes motivated by the classical problem.

The increase in the number particles n does not bring the two evolutions closer for the normalized case, but we note some possibly interesting recurrence patterns that depend on the underlying classical dynamics and on n.

Note that the classical limit for the problem is defined as the limit $n \to \infty$, with $|\gamma|n$ fixed, where γ is a parameter multiplying the nonlinear part, see e.g. [18,34,37,38]. The usual heuristic definition is in [18], while the more theoretical approach in [37,38] is based on the comparison of classical and quantum distribution functions. The convergence of the two evolution laws in that limit was also examined analytically and numerically for the trimer in [7,9]. Another comparison between classical and quantum dynamics for a related system is in [19].

Parameter γ was here set to unity, but can be introduced by suitable rescalings of δ and the time. Clearly this limit requires vanishing nonlinearity. Note that the one-peak breather can be continued for δ arbitrarily large, where it converges to the lowest frequency normal mode of the linear problem, see [14,28,29]. In that case we have localization in Fourier (normal mode) space, which is another interesting classical problem, see e.g. references in [29].

A possible understanding of the behavior of $\overline{D}(t)$ would require a comparison between the behavior of the classical trajectory on the one hand, and the eigenvalues and eigenfunctions of the quantum problem (which may be amenable to perturbation arguments in some limits, e.g. small or large $|\delta|$.) In the case of the stable one-peak classical breathers and their vicinity we would be likely comparing oscillatory evolutions with many frequencies, at both the classical and quantum level. The number of the most relevant quasi-frequencies of the quantum evolution depends on the projection of the Glauber initial state to the eigenfunctions of H. In the two-peak breather the classical trajectories have a more complicated structure, and classical recurrence is due to homoclinic behavior. Understanding the Glauber states obtained from such trajectories seems more difficult. It is possible that the differences observed in Figs. 4 (a), (b) are due to the underlying classical dynamics, i.e. the quantum evolution of the two nearby initial states is probably close in both cases, but in Fig. 4(b) the classical trajectories may be far from each other due to the instability of the breather. We hope to consider these questions in further work.

We wish to thank the anonymous referees for very helpful comments. We also acknowledge partial support from grants SEP-CONACyT 177246, PAPIIT IN103916, and FENOMEC.

References

1. L. Amico, V. Penna, Phys. Rev. Lett. **80**, 2189 (1998)
2. S. Aubry, S. Flach, K. Kladko, E. Olbrich, Phys. Rev. Lett. **76**, 1607 (1996)
3. A.G. Basile, V. Elser, Phys. Rev. E **51**, 5688 (1995)
4. L. Bernstein, J.C. Eilbeck, A.C. Scott, Nonlinearity **3**, 293 (1990)
5. P. Buonsante, R. Franzosi, V. Penna, Phys. Rev. Lett. **90**, 050404 (2003)
6. P. Buonsante, V. Penna, J. Phys. A: Math. Theor. **41**, 175301 (2008)
7. P. Buonsante, V. Penna, A. Vezzani, Phys. Rev. A **82**, 043615 (2010)
8. A. Chefles, J. Phys. A: Math. Gen. **29**, 4515 (1996)
9. A. Camacho-Guardian, R. Paredes, Laser Phys. **24**, 085501 (2014)
10. J.C. Eilbeck, P.S. Lomdahl, A.C. Scott, Physica D **16**, 318 (1985)
11. J.C. Eilbeck, F. Palmero, Phys. Lett. A **331**, 201 (2004)
12. D. Ellinas, M. Johansson, P.L. Christiansen, Physica D **34**, 126 (1999)
13. S. Flach, V. Fleurov, J. Phys.: Condens. Matter **9**, 7039 (1997)
14. R. Franzosi, S.M. Giampaolo, F. Iluminati, Phys. Rev. A **82**, 063620 (2010)
15. D.M. Gitman, A.L. Shelepin, Coherent states of the SU(N) groups, [arXiv:hep-th/9208017v1] (1992)

16. R.J. Glauber, Phys. Rev. **131**, 2766 (1963)
17. R. Goodman, J. Phys. A: Math. Theor. **44**, 425101 (2011)
18. M. Hiller, T. Kottos, T. Geisel, Phys. Rev. A **79**, 023621 (2009)
19. M.P. Jacobson, C. Jung, H.S. Taylor, R.W. Field, J. Chem. Phys. **111**, 600 (1999)
20. M. Johansson, J. Phys. A: Math. Gen. **37**, 2201 (2004)
21. T. Kapitula, P.G. Kevrekidis, Z. Chen, SIAM J. Appl. Dyn. Syst. **5**, 598 (2007)
22. P.G. Kevrekidis, *The Discrete Nonlinear Schrödinger Equation* (Springer, New York, 2009)
23. J.C. Klauder, E.G.C. Sudarshan, *Fundamentals of Quantum Optics* (W.A. Benjamin, New York, 1968)
24. W.H. Louisell, *Quantum Statistical Properties of Radiation* (John Wiley and Sons, New York, 1973)
25. R.S. MacKay, S. Aubry, Nonlinearity **7**, 1623 (1994)
26. P.D. Miller, A.C. Scott, J. Carr, J.C. Eilbeck, Physica Scripta **44**, 509 (1991)
27. P. Panayotaros, Physica D **241**, 847 (2012)
28. P. Panayotaros, Disc. Cont. Dyn. Syst. S, 1227 (2011)
29. P. Panayotaros, Phys. Lett. A **374**, 3912 (2010)
30. C.L. Pando, E.J. Doedel, Physica D **238**, 687 (2009)
31. D.E. Pelinovsky, P.G. Kevrekidis, D.J. Frantzeskakis, Physica D **212**, 1 (2005)
32. D.E. Pelinovsky, V.M. Rothos, Physica D **202**, 16 (2005)
33. R.A. Pinto, M. Haque, S. Flach, Phys. Rev. A **79**, 052118 (2009)
34. S. Raghavan, A. Smerzi, V.M. Kenkre, Phys. Rev. A **60**, 1787 (1999)
35. A.C. Scott, L. Bernstein, J.C. Eilbeck, J. Biol. Phys. **17**, 1 (1989)
36. A.C. Scott, J.C. Eilbeck, Chem. Phys. Lett. **132**, 23 (1986)
37. F. Trimborn, D. Witthaut, H.J. Korsch, Phys. Rev. A **77**, 043631 (2008)
38. F. Trimborn, D. Witthaut, H.J. Korsch, Phys. Rev. A **79**, 013608 (2009)
39. M.I. Weinstein, Nonlinearity **12**, 673 (1999)
40. E. Wright, J.C. Eilbeck, M.H. Hays, P.D. Miller, A.C. Scott, Physica D **69**, 18 (1993)